Finite-size effects on squeezing in the self-pulsing regime of second harmonic generation

Oliver Veits and Michael Fleischhauer*
Sektion Physik, Ludwig-Maximilians Universität München, D-80333 München, Germany
(Received 11 December 1996)

We analyze the quantum fluctuations of second harmonic generation at the Hopf bifurcation and in the limit-cycle regime near the critical point using many-body techniques. The many-body approach does not make use of linearization approximations and can thus be used to study finite-size effects. Finite-size corrections reduce the amount of squeezing at the Hopf bifurcation and eliminate infinities predicted by the linearization approach at this point and in the self-pulsing regime. The characteristic frequencies of the linearized fluctuation spectra in the self-oscillation regime are shifted and new spectral structures are observed. [S1050-2947(97)05606-0]

PACS number(s): 42.65.Ky

When the threshold to self-oscillations in intracavity second harmonic generation (SHG) is approached from below, the amplitude fluctuations of the two modes are reduced below the shot-noise limit [1]. Standard linearization approaches predict perfect amplitude squeezing of the fundamental (harmonic) mode if the decay rate of the fundamental mode is much larger (smaller) than that of the harmonic mode [2]. At the Hopf bifurcation itself, however, the linearization approach breaks down, since the fluctuations of the antisqueezed component diverge. Also, the region close to the bifurcation is correctly described only if the system size is infinite, i.e., in the thermodynamic limit.

The quantum noise in the self-pulsing regime above the Hopf bifurcation has been analyzed by Pettiaux, Mandel, and Fabre [3] by extending the standard linearization techniques to a nonsteady deterministic evolution. Since the fluctuation spectra show divergencies in the limit-cycle regime also, the small-noise assumption of the linearization approach is violated here as well.

Following an idea of Mertens and co-workers [4–6] and Plimak and Walls [7], we analyze here the quantum fluctuations in SHG with a many-body approach. In this approach, we numerically solve Dyson equations for Green's functions or time-ordered correlation functions in the bare-vertex approximation. Unlike Refs. [4–6], we use an iteration scheme, which starts from a mean-field approach [8] and are in this way able to achieve convergence at the Hopf bifurcation itself and in the limit-cycle regime. Since the many-body approach does not make use of small-noise assumptions, we can study the quantum fluctuations beyond the thermodynamic limit, i.e., taking into account finite-size effects.

The quantum dynamics of intracavity second harmonic generation is described by the interaction Hamiltonian [9]

$$V_{\mathrm{SHG}} = -i\hbar\frac{K}{2}(a_2 a_1^{\dagger 2} - a_2^{\dagger} a_1^2) + i\hbar\epsilon_1(a_1 - a_1^{\dagger}), \qquad (1)$$

where $a_{1,2}, a_{1,2}^{\dagger}$ are the annihilation and creation operators of the fundamental (1) and harmonic (2) modes, with frequencies ν and 2ν, and ϵ_1 describes an external coherent pumping. The nonlinear interaction between the modes is described by the coupling constant K, which is proportional to the second-order susceptibility of the nonlinear crystal and the inverse cavity volume. There are two parameters that describe the classical scale of the two modes:

$$n := \frac{\gamma_1^2}{K^2}, \quad m := \frac{2\gamma_1\gamma_2}{K^2}, \qquad (2)$$

where $\gamma_{1,2}$ are the cavity decay rates of the fundamental and harmonic mode, respectively. Normalizing the mode operators to these scales $\tilde{a}_1 := a_1/\sqrt{m}$, $\tilde{a}_2 := a_2/\sqrt{n}$ and measuring time in units of the decay rate γ_1, $\tau := \gamma_1 t$, we find the scaled Heisenberg-Langevin equations:

$$\frac{d}{d\tau}\tilde{a}_1 = -\tilde{a}_1 + \tilde{\epsilon}_1 + \tilde{a}_2\tilde{a}_1^{\dagger} + \sqrt{\frac{2}{m}}F_1(\tau), \qquad (3)$$

$$\frac{1}{\gamma}\frac{d}{d\tau}\tilde{a}_2 = -\tilde{a}_2 - \tilde{a}_1^2 + \sqrt{\frac{2}{n}}F_2(\gamma\tau). \qquad (4)$$

Here F_1 and F_2 are δ-correlated noise forces and $\tilde{\epsilon}_1 := \epsilon_1/\gamma_1\sqrt{m}$. $\gamma := \gamma_2/\gamma_1$ is the ratio of the cavity decay rates of the harmonic and fundamental mode. It also relates the two system-size parameters via $m = 2\gamma n$.

From the Langevin equations (3) and (4) and the commutation relations $[\tilde{a}_1, \tilde{a}_1^{\dagger}] = 1/m$ and $[\tilde{a}_2, \tilde{a}_2^{\dagger}] = 1/n$, one can see that in the thermodynamic limit of large system-size parameters, the field operators can be treated classically ($\tilde{a}_\mu \to \tilde{\alpha}_\mu$). The classical dynamics of SHG was studied by McNeil, Drummond, and Walls [10,11] and Mandel and Erneux [12] under conditions of a stationary external pump. For small values of the pump rate, the system has a stable steady state, where the amplitudes of the fundamental and harmonic mode are given by

$$\tilde{\alpha}_1(1 + |\tilde{\alpha}_1|^2) = \tilde{\epsilon}_1, \quad \tilde{\alpha}_2 = -\tilde{\alpha}_1^2. \qquad (5)$$

*Also at Dept. of Physics, Texas A&M University, College Station, TX 77843-4242.

When a critical value of the pump rate $\tilde{\epsilon}_1^{\rm cr}=\sqrt{1+\gamma}(2+\gamma)$ is reached, the system undergoes a Hopf bifurcation into a stable limit cycle with an oscillation frequency at threshold of $\omega_0/\gamma_1=\sqrt{\gamma(2+\gamma)}$.

In the steady-state regime below the bifurcation, standard linearization techniques [2] have shown that the amplitude fluctuations of both modes are reduced below the shot-noise or vacuum limit. In fact, perfect squeezing has been predicted at the critical point for the harmonic mode in the good converter limit $\gamma\to\infty$ or in the fundamental mode in the bad converter limit $\gamma\to 0$. However, since the fluctuations in the orthogonal field component diverge, the linearization is not valid at this point.

A linear fluctuation analysis in the limit-cycle regime near the bifurcation for the case of a good converter ($\gamma\to\infty$) was given by Pettiaux, Mandel, and Fabre [3]. This work was based on the analytic results for the deterministic limit-cycle dynamics near threshold derived in [12]. The authors found divergencies at multiples of the self-oscillation frequency in the fluctuation spectra. Since this implies diverging equal-time correlations of the fluctuations, the small-noise assumption of the linearization approach is violated in the limit-cycle regime.

We analyze here the stationary properties of intracavity SHG beyond the level of linearization, applying nonequilibrium Green's function (GF) techniques [13] in a similar way as in Ref. [14], where we have studied parametric down-conversion. For the purpose of a compact and simple notation, let us introduce here a general three-boson interaction of the form

$$V=i\hbar\frac{1}{3!}v_{klm}A_k(t)A_l(t)A_m(t)+i\hbar\epsilon_k A_k(t), \tag{6}$$

where the subscript $i\in\{m^+,m\}$ indicates that A_i creates or annihilates a photon of mode m. In the case of intracavity second-harmonic generation, we have $v_{1^+1^+2}=v_{1^+21^+}=v_{21^+1^+}=K$, and $v_{112^+}=v_{12^+1}=v_{2^+11}=-K$, and all others vanish. We introduce Green's functions or correlation functions of mode operators A_i^H in the Heisenberg picture (superscript H):

$$D_{ij}(\check{t}_1,\check{t}_2)=\langle T_C A_i^H(\check{t}_1)A_j^H(\check{t}_2)\rangle-\langle A_i^H(\check{t}_1)\rangle\langle A_j^H(\check{t}_2)\rangle. \tag{7}$$

Here, $\check{t}$ denotes a time on the so-called Schwinger-Keldysh time contour C, which goes from $t=-\infty$ via $t=+\infty$ back to $t=-\infty$ [15]. Each physical time t corresponds to two values on the contour, either on the upper $(+)$ or on the lower branch $(-)$. T_C is a time-ordering operator on C, which corresponds to time ordering T on the upper and to antitime ordering T^{-1} on the lower branch of C. In addition, it orders all operators on $(+)$ to the right of those on $(-)$. In this way, time-, antitime-, normal-, and antinormal-ordered products can be written in a simple common way. $\langle\ \rangle$ stands for $\mathrm{Tr}\{\rho_0\cdots\}$, ρ_0 being the density operator of the system at $t=-\infty$. Note that the definition (7) also contains so-called anomalous Green's functions with two annihilation or creation operators, which are needed to describe quadrature squeezing. Furthermore, mixed-type Green's-function-containing operators of different modes need to be taken into account. The (known) Green's functions without the nonlinear interaction between the modes and without external pumping are denoted by $D_{ij}^0(\check{t}_1,\check{t}_2)$.

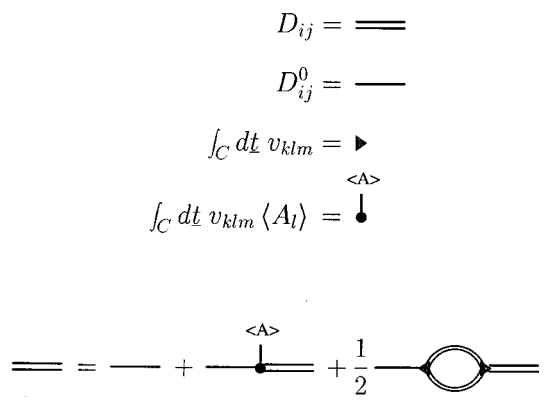

FIG. 1. Graphical representation of the Dyson equation in the bare-vertex approximation. Double lines denote the exact and single lines the known free GF. The self-energy consists of a mean-field contribution ($\sim\langle A\rangle$) and a one-loop contribution.

A relation between the unknown exact Green's functions and the known free expressions is given by the Dyson equation [13]

$$D_{ij}(\check{1},\check{1}')=D_{ij}^0(\check{1},\check{1}')+\int\int_C d\check{2}d\check{3}D_{ik}^0(\check{1},\check{2})\times P_{kl}(\check{2},\check{3})D_{lj}(\check{3},\check{1}'), \tag{8}$$

where we have used $\check{1},\check{2},\ldots$ for time arguments. P_{ij} are the so-called self-energies, which in the bare-vertex approximation [6,14] can be expressed in terms of the mean amplitude of the modes and exact GF's:

$$P_{ij}(\check{1},\check{2})=v_{ijk}\langle A_k^H(\check{1})\rangle\delta(\check{1},\check{2})+\frac{1}{2!}v_{ikl}D_{km}(\check{1},\check{2})D_{ln}(\check{1},\check{2})v_{mnj}. \tag{9}$$

A simple pictorial representation of the Dyson equation using Feynman diagrams is given in Fig. 1. Single lines represent the known free Green's functions, double lines the exact ones. At each vertex denoted by a triangle or circle, an integration over the whole Keldysh contour and a summation over all mode indices has to be performed.

The Dyson equation (8) is a nonlinear integral equation. Under stationary conditions the integrations can be reduced to one by Fourier transformation, with respect to physical (not contour) times. It should be noted that there is complete phase symmetry with respect to the limit-cycle oscillations in a quantum mechanical calculation. The mean values of the modes $\langle\tilde{a}_\mu\rangle$ are therefore time independent under conditions of stationary pump.

If only the first term of the self-energy, Eq. (9), is taken into account, the Dyson equation (7) can be solved analytically in terms of the (as yet unknown) mean amplitudes of the fields. This corresponds to a mean-field approach [8], in which the harmonic mode operator is replaced by its mean value in the equation of motion of the fundamental mode.

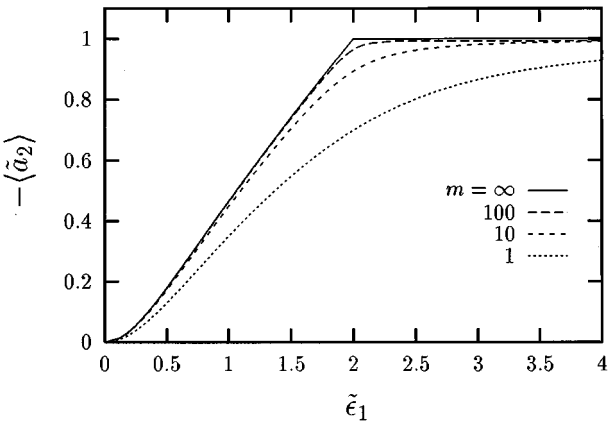

FIG. 2. Scaled mean amplitude of the harmonic mode $\langle\tilde{a}_2\rangle$ as a function of scaled pump strength $\tilde{\epsilon}_1$ from the mean-field approximation for different system-size parameters.

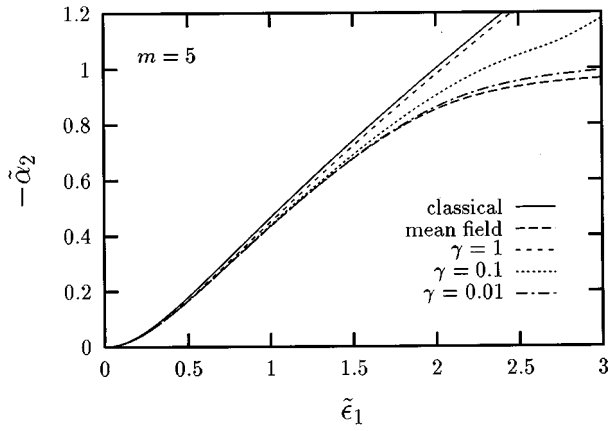

FIG. 3. Amplitude of the harmonic mode from the bare-vertex approximation for $m=5$, for different values of γ. Also shown are the classical and mean-field solutions.

One can show that this approximation remains good above the Hopf bifurcation, when the decay of the fundamental mode is much faster than that of the harmonic mode, i.e., in the bad converter limit $\gamma\to 0$ and when the system size of the harmonic mode n is kept constant. In this limit, fluctuations in the fundamental mode (more precisely, in the antisqueezed component) are short lived and do not cause fluctuations in the harmonic mode, which therefore stays quasiclassical. Also, the amplitude of the limit-cycle oscillation decreases with decreasing value of γ. Eventually, the classical trajectory $\alpha_2(t)$ lies well within the vacuum- or coherent-state uncertainty region.

In the mean-field approximation the Langevin equation (3) for the fundamental mode becomes linear in the operators and can be solved analytically in steady state. One finds

$$\langle\tilde{a}_1\rangle=\frac{\tilde{\epsilon}_1}{1-\langle\tilde{a}_2\rangle} \tag{10}$$

for the mean amplitude and

$$\langle\langle\tilde{a}_1^\dagger\tilde{a}_1\rangle\rangle=\frac{|\langle\tilde{a}_2\rangle|^2}{m(1-|\langle\tilde{a}_2\rangle|^2)},\quad \langle\langle\tilde{a}_1^2\rangle\rangle=\frac{\langle\tilde{a}_2\rangle}{m(1-|\langle\tilde{a}_2\rangle|^2)} \tag{11}$$

for the incoherent contributions to the photon number and the fluctuations $\langle\langle xy\rangle\rangle=\langle xy\rangle-\langle x\rangle\langle y\rangle$. This gives the nonlinear algebraic equation

$$-\langle\tilde{a}_2\rangle=\frac{\tilde{\epsilon}_1^2}{(1-\langle\tilde{a}_2\rangle)^2}+\frac{\langle\tilde{a}_2\rangle}{m(1-|\langle\tilde{a}_2\rangle|^2)} \tag{12}$$

for the mean amplitude of the harmonic mode, where we have assumed a real pump rate $\tilde{\epsilon}_1$. While the first term in Eq. (12) represents the classical case, the second one describes finite-size corrections and vanishes in the thermodynamic limit $m\to\infty$, except at the critical point. Due to this term, the system never reaches the critical point, as opposed to the linearization approximation, which ignores the depletion of the harmonic amplitude due to energy transfer back into fundamental fluctuations. Figure 2 shows the dependence of $\langle\tilde{a}_2\rangle$ on the external pump rate for different values of the system-size parameter. As can be seen, the harmonic-mode amplitude stays always below its critical value $\langle\tilde{a}_2\rangle=1$ (for $\gamma\to 0$) and, for small system-size parameters, the mean amplitude strongly deviates from the classical value. Equation (11) shows that the maximum squeezing is achieved only for infinite pump rates. Clearly, for any nonvanishing value of γ, the mean-field approximation becomes invalid much earlier. Analyzing corrections to the mean-field approximation, one finds that the range of validity increases when the system size m of the fundamental mode becomes small.

For finite values of γ, the mean-field results do not accurately describe the behavior at and beyond the Hopf-bifurcation and the whole bare-vertex equation needs to be solved. This is done by a numerical iteration scheme, which uses the well behaved mean-field results as a starting point [14]. This scheme is therefore also applicable at and, to a certain extent, above, the Hopf bifurcation, where linearized Green's functions are divergent. The results for the mean amplitude of the harmonic mode are shown in Fig. 3 for different values of γ. The curves approach the mean-field predictions for small values of γ and the classical result for large values of γ.

We have calculated the squeezing spectrum for the in-phase quadrature component of the fundamental mode $x_1=(a_1+a_1^\dagger)/2$:

$$S_x(\omega)=2\gamma_1\int d\tau\, e^{-i\omega\tau}\langle\langle x_1(t)x_1(t-\tau)\rangle\rangle. \tag{13}$$

The results are shown in Figs. 4 and 5 for $\gamma=0.1$ and different system-size parameters of the fundamental mode. In Fig. 4 we have chosen a pump rate just below the Hopf bifurcation, which is at $\tilde{\epsilon}_1\approx 2.203$ here. One can see that for small values of m the squeezing is reduced. Also, peaks at approximately even mutiples (here 0 and 2) of the self-oscillation frequency can be seen. This has already been noted by Mertens and Kennedy [16] in the below-threshold analysis of SHG. This feature corresponds to the peaks predicted in the above-threshold linearized spectra [3]. Since the threshold to self-oscillations is smeared out due to finite-size correction, this behavior is expected. Note, however, that the

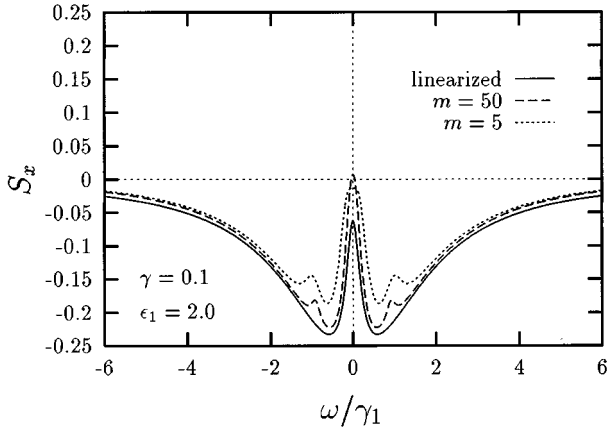

FIG. 4. Squeezing spectrum $S_x(\omega)$ of fundamental amplitude fluctuations $[x=(a_1+a_1^\dagger)/2]$ for $\gamma=0.1$ below threshold $\tilde{\epsilon}_1=2.0$ (threshold at $\tilde{\epsilon}_1\approx 2.2$), for a small and a larger system. Also shown is the linearization result from [2].

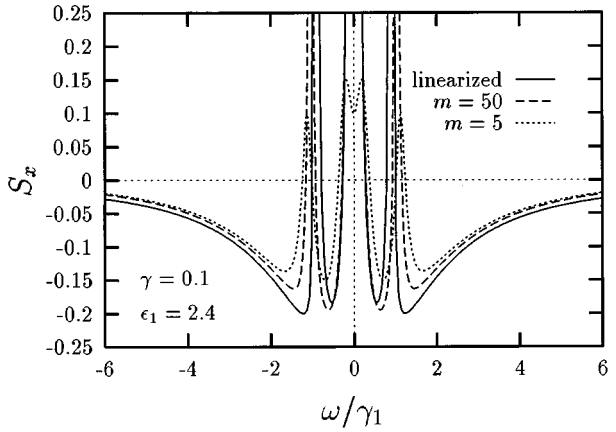

FIG. 5. Squeezing spectrum $S_x(\omega)$ of fundamental amplitude fluctuations $[x=(a_1+a_1^\dagger)/2]$ for $\gamma=0.1$ above threshold $\tilde{\epsilon}_1=2.4$ (threshold at $\tilde{\epsilon}_1=2.2$), for a small and a larger system. Also shown is the linearization result derived from analytical results for the classical limit cycle [12] following [3].

position of the peaks is shifted to higher frequencies with decreasing system size m.

Figure 5 corresponds to a point above the Hopf bifurcation. Here the peaks at even multiples of the self-oscillation frequency are much more pronounced. As opposed to the linearization result, which has been calculated along the lines of Ref. [3] and is shown here for comparision as well, these peaks have a finite height, which increases with the system size. Their position is shifted, indicating an increase of the self-oscillation frequency due to finite-size corrections.

A new spectral feature occurs in the bare-vertex spectrum above the bifurcation point. An additional splitting of the peak around $\omega=0$ can be observed for smaller values of m. This splitting is due to the finite-size renormalization of the characteristic frequencies. The characteristic frequencies of the fundamental and harmonic mode are shifted from the classical limit-cycle value by different amounts, which leads to an additional beat note.

If the pump rate is further increased, the bare-vertex approximation breaks down and higher- order terms in the vertex expansion [6,14] need to be taken into account. The breakdown occurs earlier for larger values of γ, which can be understood if we note that the present approximation corresponds to an expansion around the mode amplitudes averaged over the phase-space distribution and the phase of the limit cycle. Hence, the approach becomes less accurate as these oscillations become more pronounced. We expect, however, that an approach that allows for a spontaneous breaking of the limit-cycle phase symmetry (similar to the above-threshold parametric oscillator [14]) can overcome this problem. This will be the subject of further investigations.

O.V. thanks the Bayrisches Kultusministerium and the DAAD and M.F. thanks the Feodor-Lynen Programm of the Alexander-von-Humboldt Stiftung for financial support.

[1] Squeezing in SHG has first been demonstrated experimentally in S. F. Pereira, Min Xiao, H. J. Kimble, and J. L. Hall, Phys. Rev. A **38**, 4931 (1988).
[2] M. J. Collett and D. F. Walls, Phys. Rev. A **32**, 2887 (1985).
[3] N. P. Pettiaux, P. Mandel, and C. Fabre, Phys. Rev. Lett. **66**, 1838 (1991).
[4] C. J. Mertens, T. A. B. Kennedy, and S. Swain, Phys. Rev. Lett. **71**, 2014 (1993).
[5] C. J. Mertens, T. A. B. Kennedy, and S. Swain, Phys. Rev. A **48**, 2374 (1993).
[6] C. J. Mertens, J. Hasty, H. H. Roark III, D. Nowakowski, and T. A. B. Kennedy, Phys. Rev. A **52**, 742 (1995).
[7] L. I. Plimak and D. F. Walls, Phys. Rev. A **50**, 2627 (1994).
[8] O. Veits and M. Fleischhauer, Phys. Rev. A **52**, 4344 (1995).
[9] P. D. Drummond, K. J. McNeil, and D. F. Walls, Opt. Acta **28**, 211 (1981).
[10] K. J. McNeil, P. D. Drummond, and D. F. Walls, Opt. Commun. **27**, 292 (1978).
[11] P. D. Drummond, K. J. McNeil, and D. F. Walls, Opt. Acta **27**, 321 (1980).
[12] P. Mandel and T. Erneux, Opt. Acta **29**, 1 (1982).
[13] See, for example, L. P. Kadanoff and G. Baym, *Quantum Statistical Mechanics* (Benjamin, New York, 1962); V. Bonch-Bruevich and S. Tjablikov, *The Green's Function Method in Statistical Mechanics* (North-Holland, Amsterdam, 1962); A. L. Fetter and J. D. Walecka, *Quantum Theory of Many-Particle Systems* (McGraw-Hill, New York, 1971); D. J. Amit, *Field Theory, the Renormalization Group, and Critical Phenomena* (World Scientific, Singapore, 1984).
[14] O. Veits and M. Fleischhauer, Phys. Rev. A **55**, 3059 (1997).
[15] L. V. Keldysh, Zh. Eksp. Teor. Fiz. **47**, 1515 (1964) [Sov. Phys. JETP **20**, 1018 (1965)].
[16] C. J. Mertens and T. A. B. Kennedy, Phys. Rev. A **53**, 3497 (1996).